ECE/COE 1896

Senior Design

6 Degree of Freedom UAV Thrust Model Summary

Prepared By: *Levi Burner*

April 24, 2018

Contents

List of Figures

1 Introduction

The success of a propeller driven, autonomous aerial vehicle is tightly coupled to the accuracy of the model of its propellers used when designing the controller. This document will briefly explain the thrust model used for the 6 Degree of Freedom UAV senior design project.

The goal of this model is to characterize the response of arbitrary ESC, motor, and prop combinations using typical components found in the hobby UAV market. Controllers can then be designed with the actuator limits in mind. The model is being designed and implemented in such a way that it can be quickly use to evaluate different systems and recalculate model parameters without time consuming hand calculations.

The results in this paper are for a Sunnysky X2212 980kv motor with a generic plastic 10x4.5 propeller. However, this model can and has been applied to other propeller and motor combinations.

Many claims will be made without citation. This document is just to quickly explain the reasoning behind the thrust model to individuals familiar with the project. The model itself is the original work of the author, however, the ideal motor equations and information drawn from the general hobby RC community are clearly not original to the author.

2   Background

DC motors can be approximated by Equation (1) and Equation (2).

$$\tau = K_i I \tag{1}$$

$$I = (V - K_v \omega)/R_m \tag{2}$$

Where K_i is the motor constant relating current through the motor to torque, K_v is the motor constant relating rotation rate to back emf, and R_m is the motor's DC resistance.

By adding an inertial load I_l, the equations can be combined to form Equation 3, which is a first order ODE. This means that for a change in voltage, a first order response in rotation rate can be expected.

$$\alpha = \frac{\tau}{I_l} = \frac{K_i}{R_m} * (V - K_v \omega) \tag{3}$$

Brushless motors typically used for UAV's can be approximated identically. While their operation is significantly more complicated due to being driven by 3-phase AC generated by ESC's, it is known in the hobby community that Equations (1) and (2) still hold true. However, the loads used on UAV motors are propellers which have a non-linear thrust to rpm relationship. This affects the perceived inertial load by the motor at different operating points and when accelerating or decelerating.

3   Model Design

If a first order approximation is to be used, the response of a rotor towards a final thrust with zero initial conditions can be approximated as below.

$$T = (1 - e^{-\frac{t}{\tau_c}})T_f \tag{4}$$

A lumped parameter model can then be built from this that takes the following characteristics into account.

- Rotors appear to have different inertia at different operating points which also depends on if the thrust is be increased or decreased

- In the steady state, the output voltage corresponds to a single thrust through a monotomically increasing function

- The time constant relating the transition from the thrust associated with a voltage from another thrust is different for every combination of voltages and starting thrusts

- In a discrete model suitable for use in a robotics application the response will need to be recalculated for every timestep

- A controller needs to be able to reverse the response equation to find the voltage for a desired thrust

- Component characteristics for hobby grade UAV components are typically not published by manufacturers

Equation (5) shows a first order approximation of rotor response that does not rely on zero initial conditions. It takes the above characteristics into account through two non-linear functions the relate voltage to steady state thrust and the operating point and voltage to the time constant associated with the rise rate.

$$T_n = (1 - e^{-\frac{t_s}{E_\tau(T_{n-1}, V_n)}})(E_T(V_n) - T_{n-1}) + T_{n-1} \tag{5}$$

T_n is the output thrust for a given discrete timestep.

$E_\tau(T, V)$ is a function returning the expected instantaneous time constant describing the thrust change rate for a given voltage and thrust. In the above equation it is assumed that the update rate is high enough for the usage of the time constant for an entire timestep will have negligible effect on error.

$E_T(V)$ is a function relating the expected thrust that a given voltage corresponds to in the steady state.

t_s is the expected time between discrete updates.

This lumped parameter model is not dependent on motor constants or propeller characteristics. This is essential, because such specifications are often not published by hobby grade RC component manufacturers. The only required system characteristics $E_\tau(T, V)$ and $E_T(V)$. These can be easily measured using a thrust test stand.

Additionally, the function above is inherently discrete and can be easily reversed by using the function to compute lookup table of starting thrusts, voltages, and ending thrusts. Bilinear interpolation can then be used to interpolate between data points when searching for the voltage corresponding to a desired ending thrust and starting thrust.

4 Data Collection for Thrust Model

A thrust stand was used to measure the instantaneous thrust, battery voltage, throttle, and current for throttle transitions between all 10% throttle increments between 0-100%. Both upward and downward thrust transitions were recorded separately. The test was completely automatic and handled by an Arduino which reports its results over a serial port. Over 100 responses were recorded in this manner.

The results are automatically processed by an Python script using SciPy. Appropriate filtering, interpolation, and fitting is performed on all responses in order to determine the time constant, applied voltage, starting thrusts, and ending thrusts for each transition.

Results of Thrust Model Data Collection

Example data for a Sunnysky X2212 980kV motor with a generic plastic 10x4.5 propeller will now be shown to examplify the results of a typical propeller and motor data collection session.

An example of a typical response curve is shown in Figure 1.
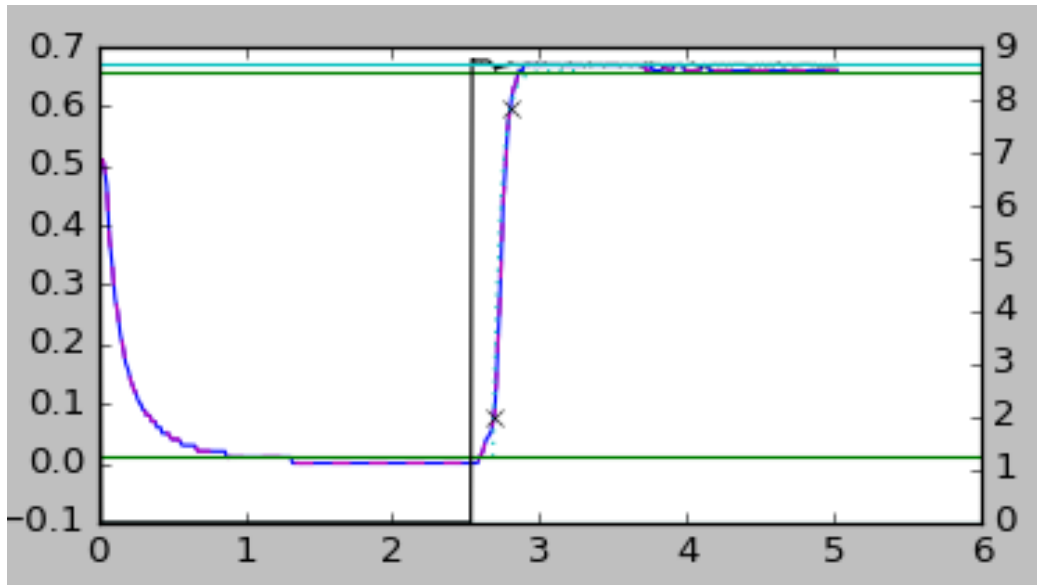

Figure 1: Typical response curve for a throttle change

In this figure the voltage (black line) was increased from 0V to approximately 8.5V. The thrust then increased from 0kg to approximately 0.65kg. The black 'x"s mark the 10% and 90% points of the thrust response. This was used to calculate the time constant for the first order approximation. The green dotted line shows the resulting first order approximation predicted thrust plotted on top of the measured values. Again, over 100 such plots were automatically generated and processed.

The ending thrusts and voltages were then used to fit a polynomial using a least square fit. A 3rd order polynomial sufficed. A polynomial was fit for both voltage to thrust and thrust to voltage. A fit is shown in Figure 2. The top curve is for voltage to thrust and the bottom is for thrust to voltage.
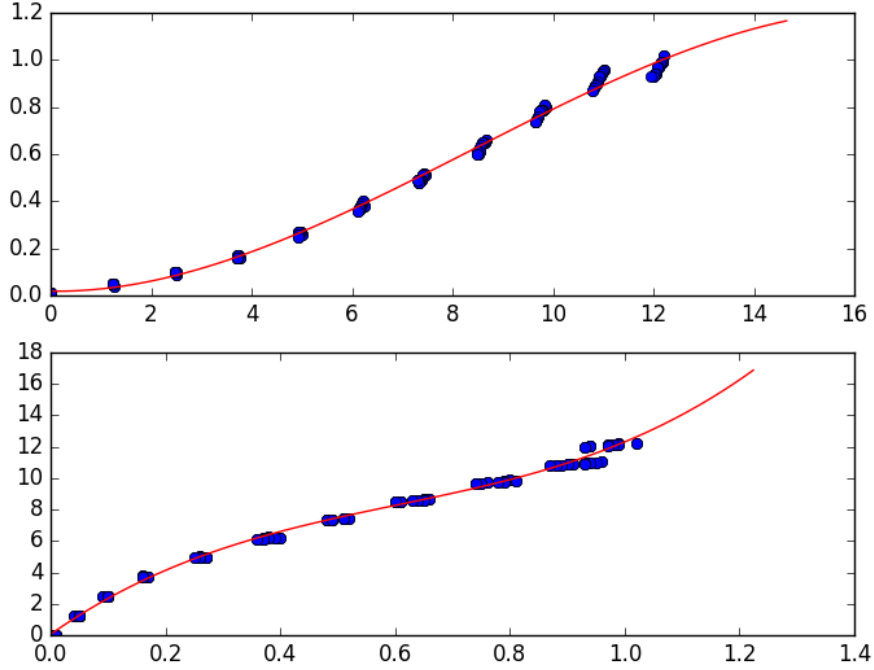
Figure 2: Voltage to Thrust and Thrust to Voltage fit

The difference between time the voltage was increased and the actual start of the thrust transition as indicated by the first order thrust approximation were used to collect data on the typical ESC response lag. This means the time the ESC takes between receiving a voltage change request and actually applying the new voltage to the motor.

A histogram showing the typical delays are shown in Figure 3. The X-axis is in seconds.
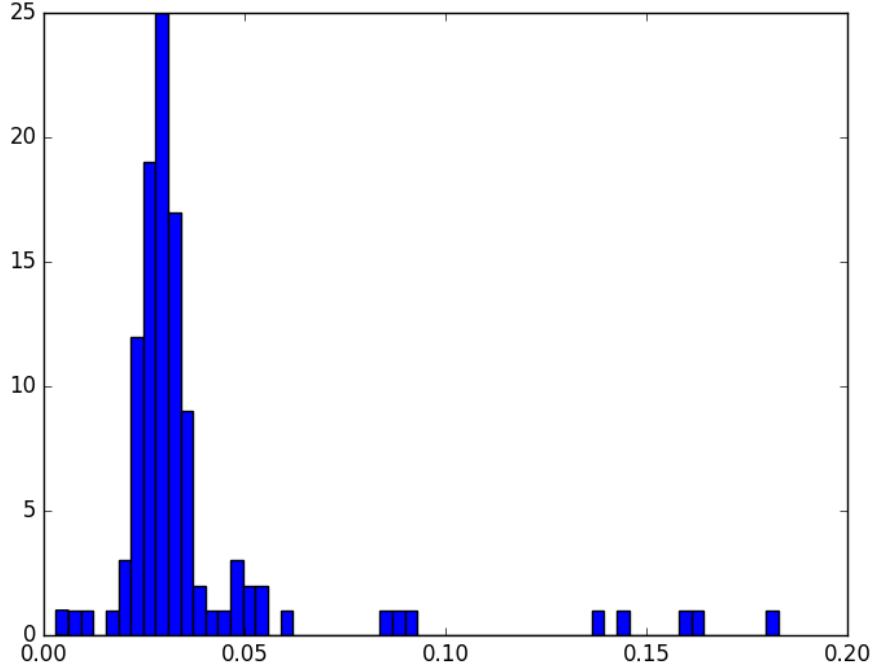
Figure 3: Histogram showing typical ESC delay

The calculated timeconstants, starting thrusts, and voltages were fit with a two polynomial surfaces. One surface was used for deceleration and another for acceleration. This is because the dynamics for deceleration are significantly different than for acceleration. Outliers were discarded by discarding time constants above a hand selected value.

The results of such a fit are in Figure 4. The Red dots are generated from the fit polynomial surface while the blue dots are actual datapoints.
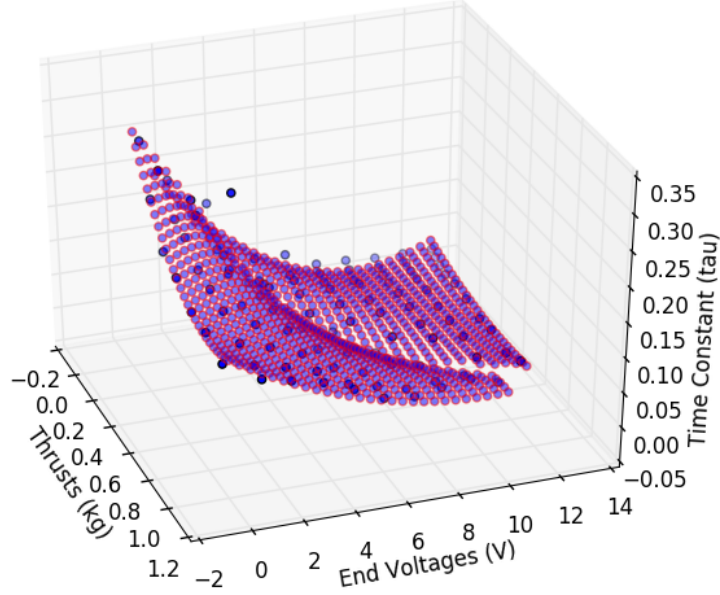
9

Figure 4: Time constant to starting thrust and voltage

In order to use the data in an actual controller a lookup table needed to be generated sot that Equation (5) could be reversed. To accomplish this the above illustrated polynomial fits were then used for $E_\tau(T, V)$ and $E_T(V)$ in Equation (5). A timestep of 20ms was used since the ESC update rate is 50Hz. The min and max voltages with some padded margins were used for voltages and the min and max thrust with some margins were used for thrusts. Points were generated for each thrust and voltage combination.

The resulting thrust model can be seen in Figure 5. The blue dots show the next achieved thrust for a given thrust and given voltage. The blue plane shows the steady state thrust achieved for a given voltage. A barely visible light blue center plane shows when the starting thrust is equal to the ending thrust.
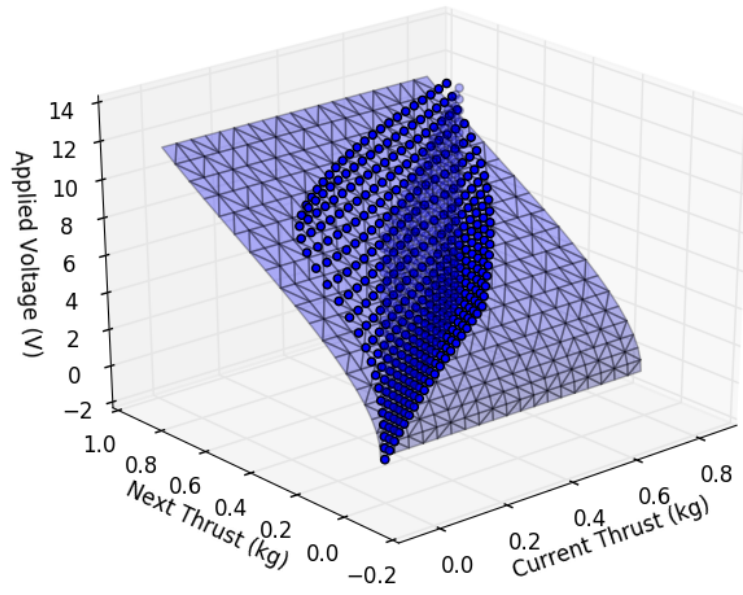
10

Figure 5: Predicted next thrust for given applied voltage and current thrust

5 Discussion of Thrust Model Data Collection

As can be seen inf Figure 1. The first order approximation aligns almost perfectly with the actual measured thrust. There was some error at the beginning and end of the response however these errors were much smaller than could be seen noticed in a typical application and were likely smaller than the accuracy of thrust in a actual use case where the the desired thrust is constantly changing.

Figure 2 shows a surprisingly linear relationship between voltage and thrust in the typical operating range of a 1 to 1.5kg drone. This explains why linear PID controllers work so well on hobby drones. However, as the edge of the operating range is approached, the relationship becomes non-linear.

The histogram of ESC delays in Figure 3 shows that the vast majority of delays are between 20-35ms. This is useful information for controllers that need to be able to predict when control effort will actually be applied.

The time constant fit shown in Figure 4 appears to work well for medium to high end voltages but low voltages and low start thrusts appear to cause inconsistent and jumpy time constants. This appeared to throw the time constant least squares fit off slightly. However not enough to be greatly concerned. Removing outlier time constants that were too high helped the fit significantly.

Finally, Figure 5 shows the relationship between the next possible thrust for a given starting thrust. As expected the higher the current thrust, the slower a prop can increase its thrust. This is due to the inherent limitations of having a maximum battery voltage. Similarly, the higher the operating thrust the quicker the thrust can be decreased as drag takes away energy from the propeller faster. The modeled limits can be used in a search based motion planner or similar if it were to plan in the jerk space.

6   Data Collection for Testing Thrust Model

In order to test the thrust model code was written to allow the thrust model lookup table to be used on the thrust test stand alluded to previously. The goal was to show the max slew rate of the propeller and motor by making it follow a trapezoidal desired thrust profile.

A trapezoidal profile was used instead of a triangular profile so that the propellers thrust value could stabilize during the flat sections of the profile.

For the Sunnysky X2212 with a generic 10x4.5 plastic propeller tests were run with 1.25, 2.5, 5, 10, 20, and 40 kg/s slew rates. Tests were run for ramps going from min to max thrust with 5% and 25% margins. Additionally tests were run using the both the thrust model shown in Figure 5 and using the thrust to voltage curve in Figure 2. This showed the difference in lag between the model that takes response time into account and a model that assumes steady state.

When using the time based thrust model if the desired thrust was within 1% of the maximum thrust range the static model was used to assign the output voltage. This is because the static model is more accurate for steady thrust because it does not rely on interpolation between pre-computed thrust points.

When calculating the output of the dynamic thrust model the current thrust was set to the last requested thrust regardless of whether or not the thrust model predicted the thrust to be possible. This was done because the model was not accurate enough to allow it to cumulatively use its last predicted thrust as the current thrust. The accumulation of error caused the model to excessive undershoot of the measured thrust compared to the target thrust.

Additionally, the steady state accuracy was tested by setting output thrusts with long time delays between transitions.

7 Results of Testing Thrust Model

The results of testing the trapezoidal motion profiles for the before mentioned tests are shown in Figures 6, 7, 8, and 9. The lag as calculated using the auto correlation, RMS error after applying the time shift maximum gain, and max error are included on each plot.

The red line is the thrust profile, the blue line is the resulting thrust, and the pink line is the error after applying the time shift found using the auto correlation.

The right vertical axis is the thrust and the left vertical axis is the thrust error. The horizontal axis is time in seconds.

The bottom figure in this section, Figure 10 shows the steady state response test.
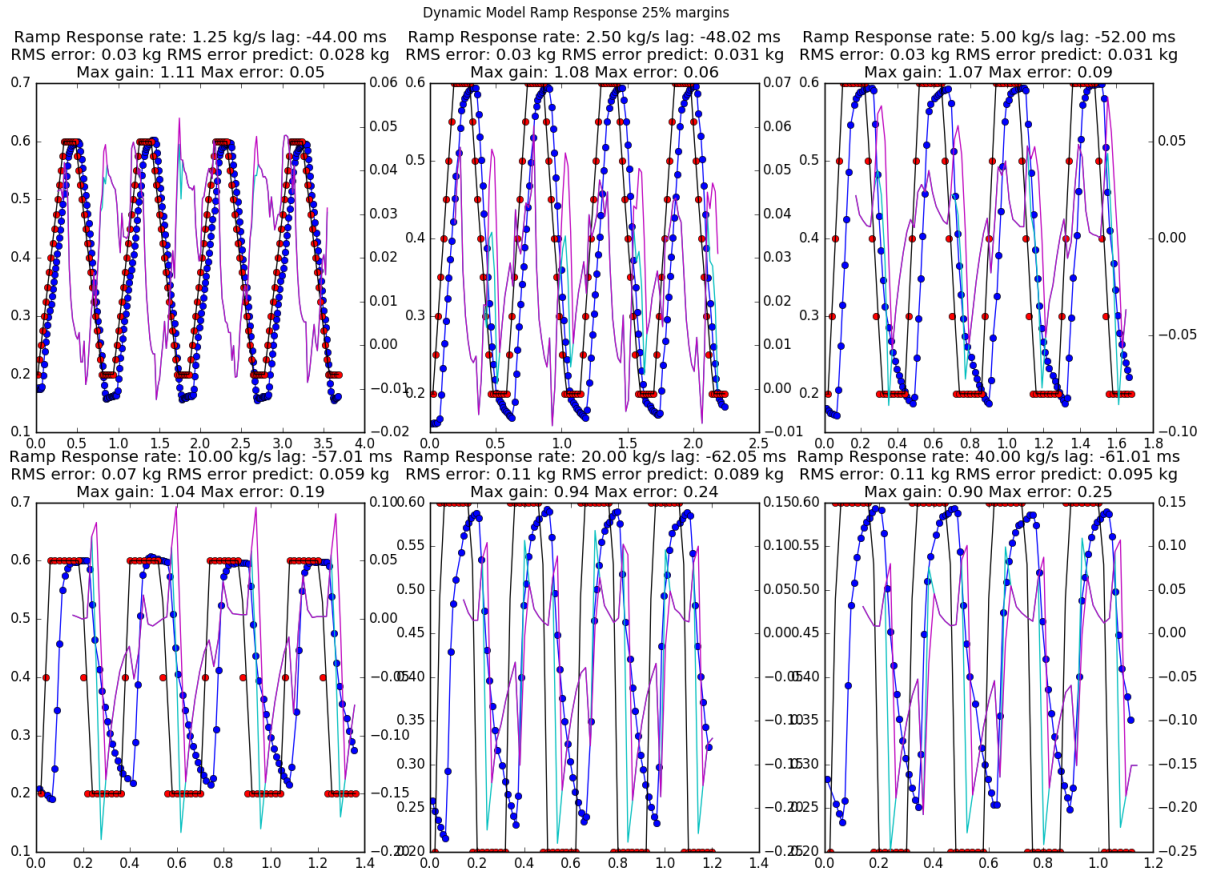
Figure 6: Desired thrust versus measured thrust for the dynamic thrust model with 25% thrust margins
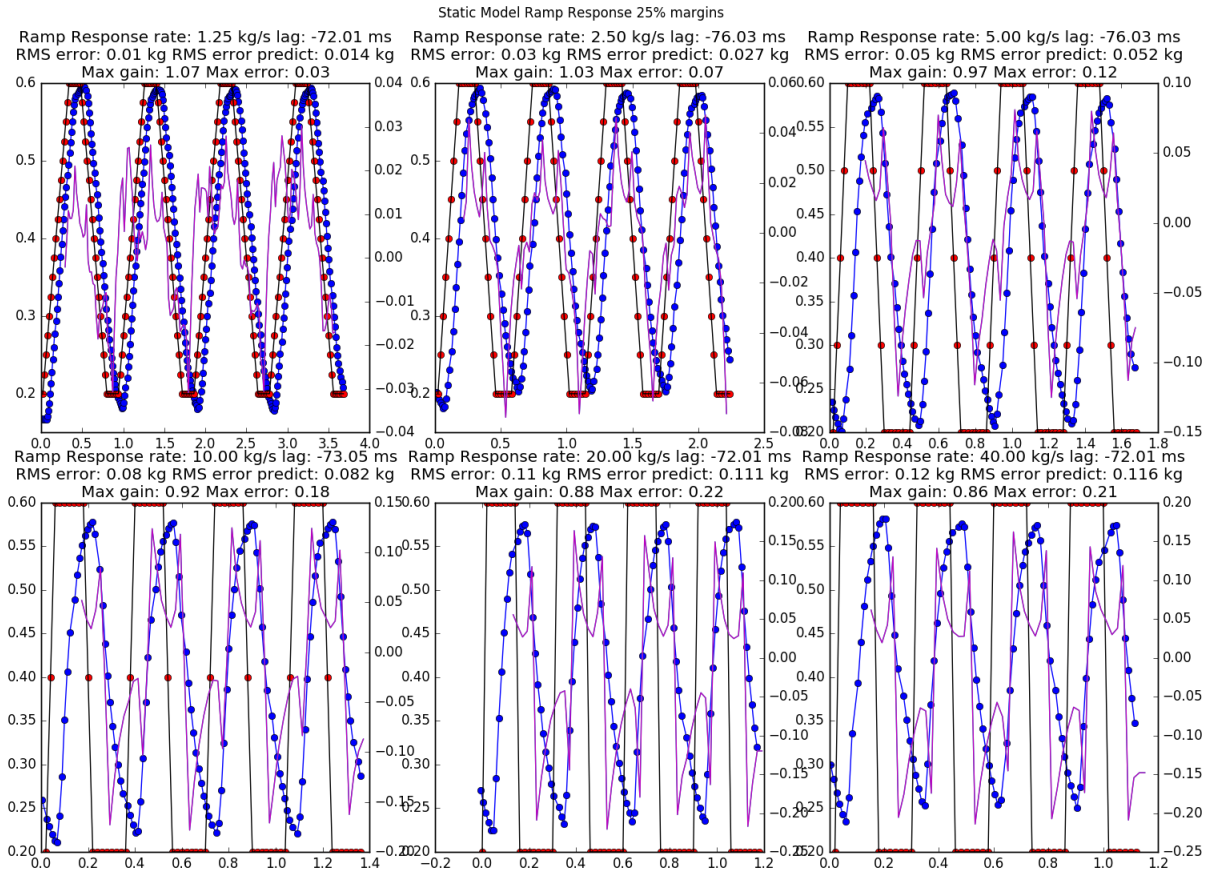
Figure 7: Desired thrust versus measured thrust for the static thrust model with 25% thrust margins
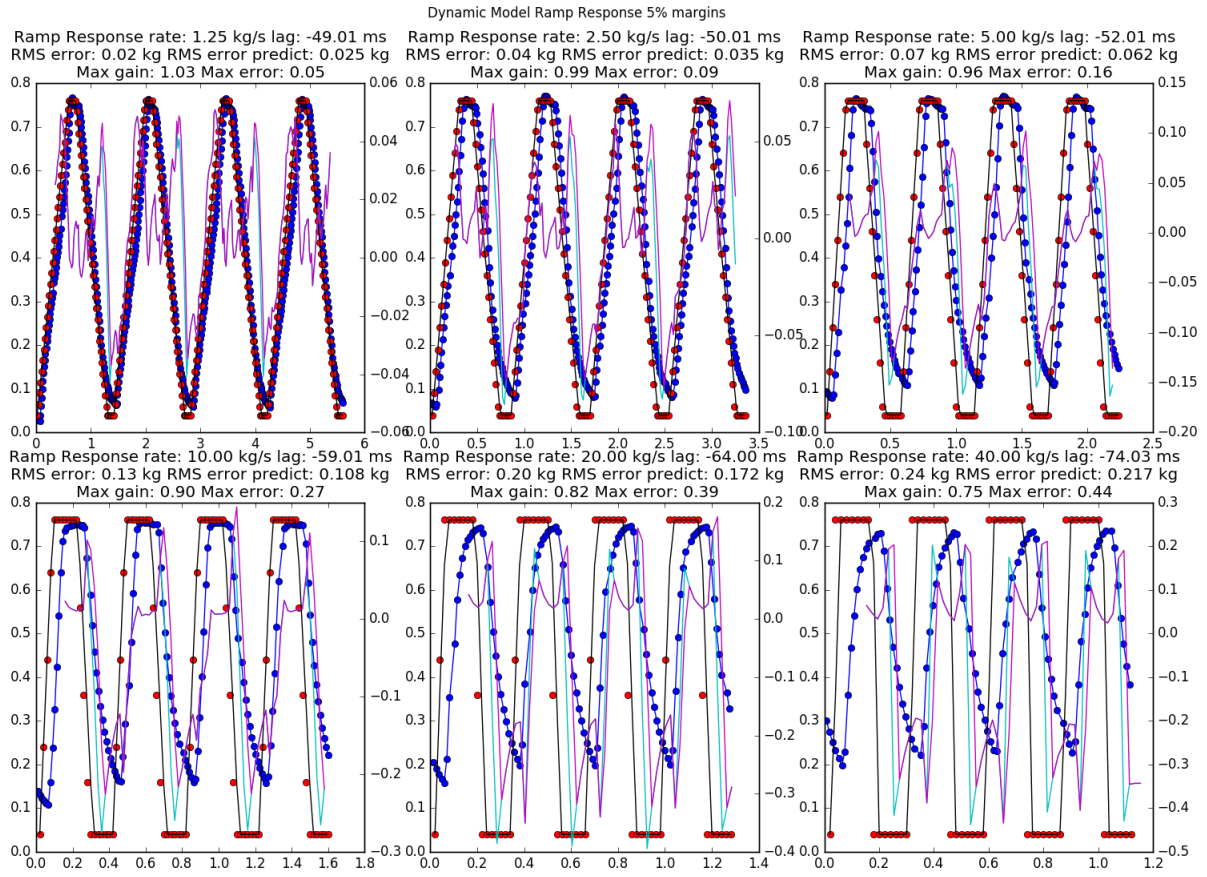
Figure 8: Desired thrust versus measured thrust for the dynamic thrust model with 5% thrust margins
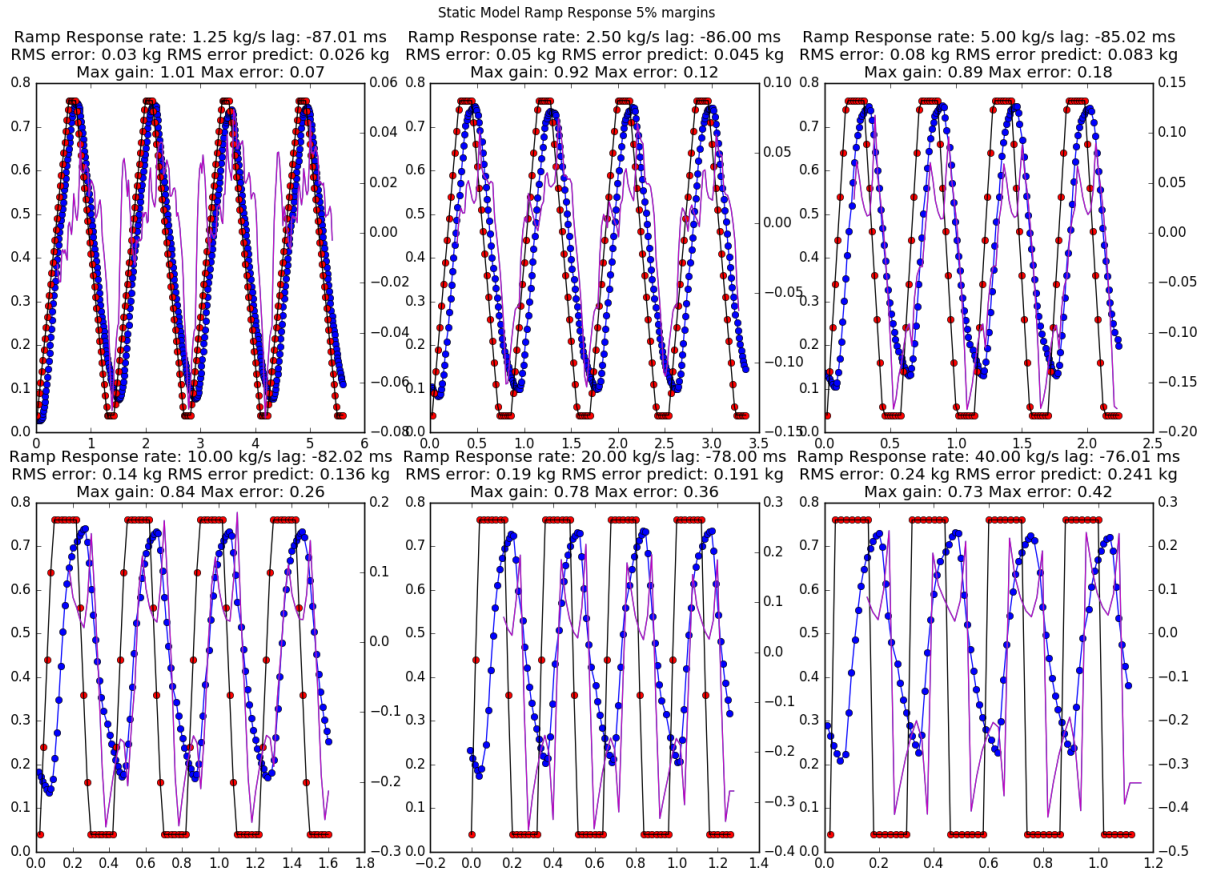
Figure 9: Desired thrust versus measured thrust for the static thrust model with 5% thrust margins
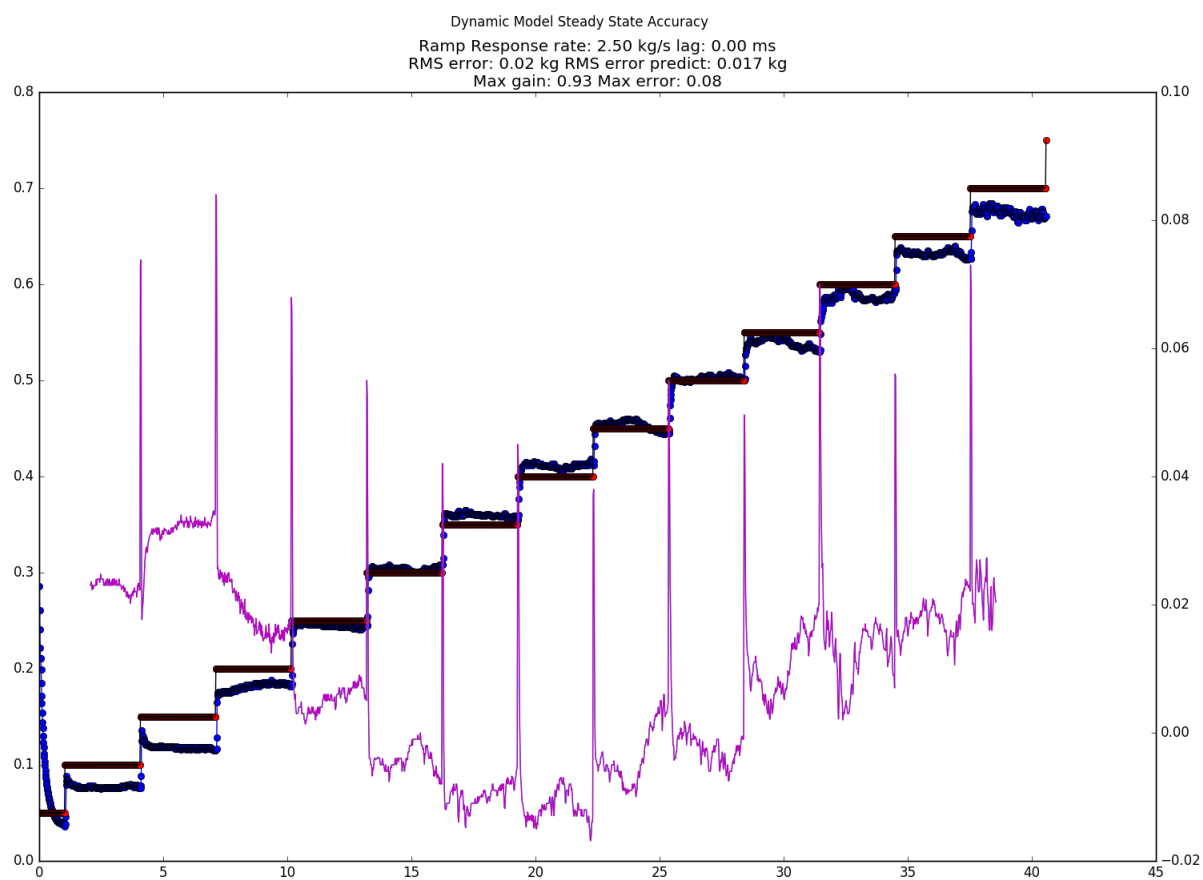
Figure 10: Steady state response of thrust model

8   Discussion of Testing Thrust Model

Figures 6, 7, 8, and 9 show that the dyanmica thrust model greatly decreases the response time of the rotor. For instance, in equivalent tests of 2.5 kg/s ramps with 5% margins the max gain of the static model was 0.92 when compared to the desired amplitude and hte lag was 86ms. Meanwhile the dynamic model achieved a gain of 0.99 with a lag of 50ms.

The 5% margin tests clearly hit the limits of the rotors ability to spin up and down regardless of thrust model. However, the 25% margins revealed that dynamic model greatly increases the max slew rate possible. The dynamic model did not drop below a max gain of 1 until 20kg/s slew rates while the static model dropped below a max gain of 1 at only 5 kg/s. Additionally, the dynamic model reduced the lag by 25-30ms typically.

Finally, Figure 10 shows that the model had a maximum steady state error of approximately 30 grams. Surprisingly this occurs at low thrusts while at higher thrusts the error is usually below 20 grams. On a 2kg drone, these 4 of these propellers would be used as the main thrust rotors. Thus the max thrust error in the steady state would be 120g or 0.588 m/s^2.

However, the typical operating range of 2kg drone is 500 grams of thrust per rotor. The error in that region is bounded by 20 grams per rotor resulting in max acceleration error of 0.392 m/s^2. These accelerations are much lower than those typically requested of a UAV in flight and can easily be fixed with an integration term in the controller.

What wasn't well researched is the power consumption of the dynamic model versus the static model. The dynamic model must use significantly more power than the static model because it raises the voltage higher in order to induce a faster response rate. However, how much more is current unknown.

9 Conclusion

The thrust model clearly decreases lag, increases maximum slew rate, and increases the accuracy during sharp thrust transitions. Additionally, this model can characterize any hobby ESC, motor, and propeller combination without requiring any knowledge of the manufacturer specifications. Since all data processing is mostly automatic it can be applied quickly to different combinations in order to evaluate performance.

The parameters derived from this model are important to all aspects of an autonomous UAV's software. Having repeatable and known statistics eases controller design significantly and takes the guess work out of motion planning. Overall, this model is expected to improve the performance of the 6 DOF UAV, especially with the side rotors.